Dynamical processes at surfaces: Excitation of electron-hole pairs

B. N. J. Persson
IBM Thomas J. Watson Research Center, Yorktown Heights, New York 10598
and Institut für Festkörperforschung, Kernforschungsanlage Jülich, D-5170 Jülich, W. Germany

S. Andersson
Department of Physics, Chalmers University of Technology, S-412 96 Göteborg, Sweden
(Received 17 October 1983)

We study the dynamical response of metal surfaces to external electric fields which vary slowly in space and time. It is shown that a linear response function $g(q_{||},\omega)$ determines the influence of a metal surface on all dynamical processes occurring outside of it. We evaluate $g(q_{||},\omega)$ approximately within the jellium model and compare the result with electron-energy-loss measurements on Cu(100) and Ni(100). Good agreement between theory and experiment is obtained, particularly for Cu(100). Finally, we give illustrative applications to the frictional force on a charged particle and the damping of excitations at surfaces.

I. INTRODUCTION

Dynamical processes at surfaces is a subject of great importance. For example, the entire field of heterogeneous catalysis, as well as many aspects of photochemistry and electrochemistry at metal surfaces, are direct manifestations of the interaction between external molecules and a surface. However, surface processes are also interesting in their own right and have a high intrinsic value to basic knowledge in physics.

Dynamical processes involving chemisorbed molecules, such as dissociation reactions[1] or vibrational damping,[2] are interesting but complicated. When a chemisorption bond is formed, some of the electrons in the system are shared between the molecule and the metal, generally leading to a nonzero charge transfer.[3] If the molecule is involved in a dynamical process (e.g., sticking or vibrational damping), time-dependent charge rearrangements will take place, which, owing to the continuum of levels at the Fermi surface of a metal, often are accompanied by strongly nonadiabatic processes.

Another class of dynamical processes involves molecules not in direct contact with the substrate surface or at least where the overlap can be neglected, as, perhaps, is the case in most physisorption systems. These processes are, of course, much simpler, because such molecules can interact with the metal only through the electromagnetic field. Interesting examples of this type include the van der Waals interaction between a molecule and a metal,[4,5] and the flourence decay of an excited molecule studied as a function of the distance to the surface.[6]

In this work we will consider problems of the latter type It will be shown that a linear response function $g(q_{||},\omega)$ exists, which completely determines the interaction between a metal surface and an external molecule, atom or charged particle. In general, all the elementary excitations of the metal such as electron-hole pairs and phonons will contribute to the structure of $g(q_{||},\omega)$. In Sec. II we consider the electron-hole pairs and present a simple analytical formula for Img which is valid for small $q_{||}$ and ω (i.e., $q_{||} \ll k_F$ and $\omega \ll \omega_F$, where k_F and ω_F is the Fermi wave number and frequency, respectively). Also in Sec. II we show that Img can be measured directly using inelastic electron scattering, and that such measurements performed on Cu(100) and Ni(100) compare favorably with theory for $\omega > \omega_0$ where ω_0 is the highest phonon frequency of the metal. For $\omega < \omega_0$, phonons will also contribute to Img, but this will not be discussed in the present work.

In Sec. III several illustrative applications of the response function $g(q_{||},\omega)$ are given. We first discuss the inelastic scattering of electrons from surfaces and make a few comments on the friction force on a charged particle at a surface. Next we discuss the quenching of excited states above surfaces. Section IV contains a summary of the most important results obtained in this work.

II. EXCITATION OF ELECTRON-HOLE PAIRS

A. Definition of $g(q_{||},\omega)$

Let a metal occupy the half-space $z > 0$ and consider an arbitrary electric current density located in the half-space $z < -d (< 0)$ as chematically shown in Fig. 1. Assume for simplicity that retardation effects can be neglected. Thus the electric field from the external current density can be written as $\vec{E}_{ext} = -\vec{\nabla}\phi_{ext}$. Since $\nabla^2\phi_{ext} = 0$ for $z > -d$, ϕ_{ext} can, in this region of space, be written as a superposition of evanescent plane waves,

$$\phi_{ext}(\vec{x}t) = \int d^2q_{||} d\omega \, \tilde{\phi}_{ext}(\vec{q}_{||},\omega) e^{i\vec{q}_{||}\cdot\vec{x}_{||} - q_{||}z - i\omega t} .$$

This external potential induces a current density in the metal which gives rise to an induced potential $\phi_{ind}(\vec{x}t)$. Assume that ϕ_{ext} is so weak that the metal responds linearly to ϕ_{ext}. For $z < 0$, where $\nabla^2\phi_{ind} = 0$, we can then write

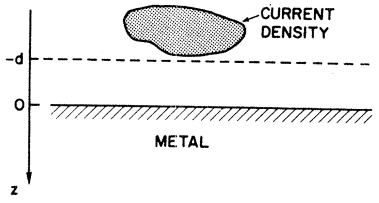

FIG. 1. Schematic representation of a current distribution above a metal surface.

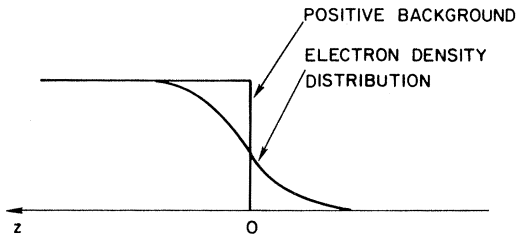

FIG. 2. Schematic representation of the density distributions.

$$\phi_{\text{ind}}(\vec{x}t)=\int d^2q_{||}d\omega[-g(q_{||},\omega)]\tilde{\phi}_{\text{ext}}(\vec{q}_{||},\omega)\times e^{i\vec{q}_{||}\cdot\vec{x}_{||}+q_{||}z-i\omega t}. \quad (1)$$

It is implicitly understood that the metal can be treated as being translationally invariant parallel to the surface. Equation (1) shows that the response of the metal to an external probe is entirely contained in $g(q_{||},\omega)$ as long as we are only interested in the induced potential outside the metal.

In the standard textbook treatment of the dielectric response of a metal surface, one assumes that the solid is characterized by a local dielectric function $\epsilon(\omega)$ which jumps discontinuously at the surface, i.e., $\epsilon=\epsilon(\omega)$ for $z>0$ and $\epsilon=1$ for $z<0$. From the continuity of $\epsilon\, d\phi/dz$ and ϕ at the solid-vaccum interface, one obtains the standard textbook result,

$$g(q_{||},\omega)=\frac{\epsilon(\omega)-1}{\epsilon(\omega)+1}. \quad (2)$$

A real metal does not have a steplike surface profile, but rather a profile which varies smoothly on a microscopic scale. In addition, the bulk dielectric function depends on the wave vector $\vec{q}$. Thus Eq. (2) is, in general, not correct, although one can prove that it is exact for $q_{||}=0$. In what follows we will show that it is possible to derive a simple but still quite accurate expression for $\text{Im}g(q_{||},\omega)$ which is valid for small $q_{||}$ and ω.

B. Qualitative discussion

In the following two sections we will present a derivation of $\text{Im}g(q_{||},\omega)$ which is valid for small $q_{||}$ and ω. Here we would like to make a few comments on the basic approach. We assume that the metal can be treated within the jellium model, i.e., the metal conduction electrons are assumed to move in a semi-infinite positive background obtained by smearing-out the positive metal-ion cores (see Fig. 2). Let us consider the response of this jellium metal to an external time-varying potential of the form

$$\phi_{\text{ext}}=\phi_0 e^{i\vec{q}_{||}\cdot\vec{x}_{||}-q_{||}z-i\omega t}+\text{c.c.}.$$

This external potential induces a charge density in the metal which gives rise to the induced potential ϕ_{ind}. The time-varying potential $\phi=\phi_{\text{ext}}+\phi_{\text{ind}}$,

$$\phi(\vec{x}t)=\phi(\vec{x})e^{-i\omega t}+\text{c.c.}, \quad (3)$$

will excite electron-hole pairs in the metal at a rate which is given by the golden-rule formula,

$$w=\frac{2\pi}{\hbar}\int d^3k\, d^3k'\, n_k(1-n_{k'})\,|\langle\vec{k}'|e\phi(\vec{x})|\vec{k}\rangle|^2\times\delta(\epsilon_{k'}-\epsilon_k-\hbar\omega), \quad (4)$$

where

$$n_k=\begin{cases}1 \text{ if } k<k_F,\\ 0 \text{ if } k>k_F,\end{cases}$$

where k_F is the Fermi wave number and where $\langle\vec{x}|\vec{k}\rangle\sim e^{i\vec{k}_{||}\cdot\vec{x}_{||}}\psi_{k_z}(z)$ are the single-particle wave functions for electrons moving in an effective one-particle potential $V_{\text{eff}}(z)$. Now, let us decompose ϕ into a surface component ϕ_{surf} plus a bulk component ϕ_{bulk}, i.e.,

$$\phi=\phi_{\text{surf}}+\phi_{\text{bulk}}.$$

Figure 3 illustrates the decomposition: $\phi=\phi_{\text{bulk}}$ for $z>\delta$, and $\phi=\phi_{\text{surf}}$ for $z<\delta$ where $z=\delta\sim$ a few Å, a point just inside the jellium edge. The matrix element $\langle\vec{k}'|\phi|\vec{k}\rangle$ occurring in Eq. (1) can now be written as

$$\langle\vec{k}'|\phi|\vec{k}\rangle=\langle\vec{k}'|\phi_{\text{surf}}|\vec{k}\rangle+\langle\vec{k}'|\phi_{\text{bulk}}|\vec{k}\rangle.$$

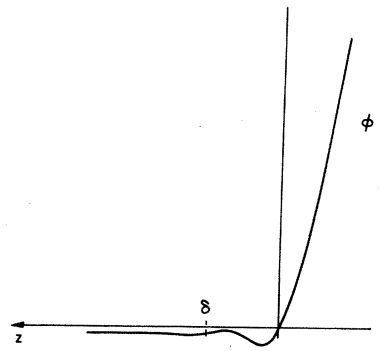

FIG. 3. Schematic representation of the electric potential ϕ (equal to external plus induced potential) in the surface region of a metal due to an external current distribution. $\phi=\phi_{\text{surf}}$ for $z<\delta$ and $\phi=\phi_{\text{bulk}}$ for $z>\delta$.

We have performed this decomposition for two reasons. First, the bulk term $\langle \vec{k}' \mid \phi_{\text{bulk}} \mid \vec{k} \rangle$ is (for $\omega \ll \omega_F$) very insensitive to the exact shape of the electron wave functions in the surface region of the metal. Thus it can be accurately evaluated using, e.g., wave functions obtained from the infinite-barrier model. This will be discussed further in subsection D. The surface term $\langle k' \mid \phi_{\text{surf}} \mid \vec{k} \rangle$, on the other hand, depends, of course, on the detailed form of the wave functions in the surface region of the metal. This term is nevertheless rather easy to evaluate, since it involves a very small region in z.

It will be shown later that

$$w \approx w_{\text{surf}} + w_{\text{bulk}} ,$$

where w_{surf} (w_{bulk}) is obtained by replacing ϕ in Eq. (4) with ϕ_{surf} (ϕ_{bulk}). Thus there is negligible interference between "surface excitation" and "bulk excitation" of electron-hole pairs. The basic reason for this is that the matrix element $\langle \vec{k} \mid \phi_{\text{surf}} \mid \vec{k} \rangle$ is sharply peaked at $k_z = k_F$, while the matrix element $\langle \vec{k} \mid \phi_{\text{bulk}} \mid \vec{k} \rangle$ is a much more smoothly varying function of k_z.

We close this section by mentioning that Img can be obtained directly from w via

$$\text{Img} = \pi \hbar w / (\mid \phi_0 \mid^2 A q_{\parallel}) ,$$

where A is the metal surface area. This formula is easily proven by integrating the normal component of the pointing vector over the metal surface and equating this with the power absorption $\hbar\omega w$.

C. Surface contribution to Img

We will now calculate the surface contribution to $\text{Img}(q_{\parallel},\omega)$ for $q_{\parallel} \ll k_F$ and $\omega \ll \omega_F$. The metal will be treated within the jellium approximation (see Fig. 2) (see also Refs. 7 and 8).

The rate w_{surf} at which the potential

$$\phi_{\text{surf}}(\vec{x},t) = \phi_{\text{surf}}(\vec{x}) e^{-i\omega t} + \text{c.c.}$$

excites electron-hole pairs in the metal is given by the golden-rule formula,

$$w_{\text{surf}} = \frac{2\pi}{\hbar} \int d^3k \, d^3k' \, n_k (1 - n_{k'}) \mid \langle \vec{k}' \mid e\phi_{\text{surf}}(\vec{x}) \mid k \rangle \mid^2 \times \delta(\epsilon_{k'} - \epsilon_k - \hbar\omega) . \tag{5}$$

The potential ϕ_{surf} can for small ω and $q_{\parallel}$ be calculated as follows: If the metal is treated classically, then

$$\nabla^2 \phi_{\text{surf}} = -4\pi \sigma(\vec{x}_{\parallel}) \delta(z) , \tag{6}$$

where $\sigma(\vec{x}_{\parallel})$ is the surface charge density. For an external potential of the form

$$\phi_{\text{ext}} = \phi_0 e^{i\vec{q}_{\parallel} \cdot \vec{x}_{\parallel} - q_{\parallel} z - i\omega} + \text{c.c.} ,$$

one obtains

$$\sigma(\vec{x}_{\parallel}) = -\frac{1}{2\pi} \frac{\epsilon(\omega) - 1}{\epsilon(\omega) + 1} q_{\parallel} \phi_0 e^{i\vec{q}_{\parallel} \cdot \vec{x}_{\parallel}} ,$$

and, for $\omega \ll \omega_p$,

$$\sigma(\vec{x}_{\parallel}) \approx -\frac{1}{2\pi} q_{\parallel} \phi_0 e^{i\vec{q}_{\parallel} \cdot \vec{x}_{\parallel}} + \text{c.c.} . \tag{7}$$

For $\omega \ll \omega_p$ the metal conduction electrons can almost respond adiabatically to the slowly varying external field, and thus almost adjust themselves to the instantaneous static configuration. Thus, to a good approximation, the potential ϕ_{surf} is obtained from a static calculation. We therefore replace Eq. (6) with

$$\nabla^2 \phi_{\text{surf}} = -4\pi \sigma(\vec{x}_{\parallel}) f(z) ,$$

where

$$\int_{-\infty}^{\infty} dz \, f(z) = 1 .$$

Since the variation of $f(z)$ with z is much more rapid than the variation of $\sigma(\vec{x}_{\parallel})$ with $\vec{x}_{\parallel}$ (the ratio is $\sim q_{\parallel}/k_F \ll 1$), we obtain

$$\phi_{\text{surf}} \approx \sigma(\vec{x}_{\parallel}) A(z) , \tag{8}$$

where

$$\frac{d^2 A}{dz^2} \simeq -4\pi f(z) . \tag{9}$$

Thus the potential ϕ_{surf} is obtained from Eq. (8) with $\sigma(\vec{x}_{\parallel})$ given by Eq. (7) and $A(z)$ calculated from Eq. (9).

We can write the electronic wave functions as

$$\langle \vec{x} \mid \vec{k} \rangle = \frac{1}{2\pi} \left[\frac{2}{\pi} \right]^{1/2} e^{i\vec{k}_{\parallel} \cdot \vec{x}_{\parallel}} \psi_{k_z}(z) , \tag{10}$$

where

$$\psi_{k_z}(z) \to \cos(k_z z + \phi_k) \quad \text{as } z \to \infty .$$

From Eqs. (8) and (10) we obtain

$$\langle \vec{k}' \mid \phi_{\text{surf}} \mid \vec{k} \rangle = -\frac{q_{\parallel} \phi_0}{2\pi} \frac{4}{(2\pi)^3} \int d^3x \, e^{i(\vec{k}_{\parallel} + \vec{q}_{\parallel} - \vec{k}'_{\parallel}) \cdot \vec{x}_{\parallel}} \times \psi^*_{k'_z}(z) A(z) \psi_{k_z}(z)$$

$$= -\frac{q_{\parallel} \phi_0}{\pi^2} \delta(\vec{k}_{\parallel} + \vec{q}_{\parallel} - \vec{k}'_{\parallel}) \langle \psi_{k'_z} \mid A \mid \psi_{k_z} \rangle .$$

Substituting this into Eq. (5) and making use of the formula

$$\mid \delta(\vec{k}_{\parallel}) \mid^2 = \frac{A}{(2\pi)^2} \delta(\vec{k}_{\parallel}) ,$$

where A is the surface area, gives

$$w_{\rm surf}=\frac{2\pi}{\hbar}\left|\frac{q_{||}e\phi_0}{\pi^2}\right|^2\frac{A}{(2\pi)^2}\int d^3k\,d^3k' n_k(1-n_{k'})\delta(\vec{k}_{||}+\vec{q}_{||}-\vec{k}'_{||})\delta(\epsilon_k+\hbar\omega-\epsilon'_k)\,|\langle\psi_{k'_z}|A|\psi_{k_z}\rangle|^2$$

$$=\left|\frac{q_{||}e\phi_0}{\pi^2}\right|^2\frac{A}{2\pi\hbar}\frac{m}{\hbar^2}\int d^3k\,n_k(1-n_{k'})\frac{1}{k'_z}\,|\langle\psi_{k'_z}|A|\psi_{k_z}\rangle|^2 . \tag{11}$$

Performing the integration over k and accounting for the electron spin (which introduces an extra factor of 2) gives

$$w_{\rm surf}\approx\frac{2}{\pi^4}\left[\frac{me}{\hbar^2}\right]^2 A\,|\phi_0|^2 q_{||}^2\omega \times\int_0^{k_F}dk_z\frac{1}{k_z}\,|\langle\psi_{k_z}|A|\psi_{k_z}\rangle|^2 . \tag{12}$$

Since

$$\mathrm{Img}=\pi\hbar w/(|\phi_0|^2 A q_{||}) ,$$

we have

$$(\mathrm{Img})_{\rm surf}\approx 2\frac{q_{||}}{k_F}\frac{\omega}{\omega_p}\xi(r_s) , \tag{13}$$

where

$$\xi(r_s)=\frac{1}{8\pi^2}\frac{\omega_p}{\omega_F}\left[\frac{k_{\rm TF}}{k_F}\right]^2\int_0^{k_F}dk_z\frac{1}{k_z}\,|\langle\psi_{k_z}|Ak_F^2|\psi_{k_z}\rangle|^2 , \tag{14}$$

where $k_{\rm TF}^{-1}$ is the Thomas-Fermi screening length. In the jellium model, ξ depends only on the electron-gas density parameter r_s; $\xi(r_s)$ has been calculated in Refs. 5 and 7.

The calculation presented above is simple and it is easy to extract some interesting physics from it.[7] Note first that only electrons within a thin shell $\epsilon_F-\hbar\Omega<\epsilon<\epsilon_F$ near the Fermi surface can be excited without violating energy conservation. This does not mean that electrons in deeper-lying levels are unimportant since they will give a contribution to the screening of the external potential. Of the electrons in the vicinity of the Fermi surface, only those which propagate normal or almost normal to the metal surface will couple to the screened dipole field. The reason is that $\phi_{\rm surf}$ vanishes very rapidly inside the metal. Thus for a metal electroon to "feel" this potential, its wave function must penetrate far enough into the vacuum, and only electrons with a large velocity normal to the metal surface can do so. This is illustrated in Figs. 4 and 5. Figure 4 shows the potential $\phi_{\rm surf}$ as a function of z. Also shown are two conduction-electron wave functions, one corresponding to an electron propagating almost parallel to the surface ($k_z=0.1k_F$), and the other normal to the surface ($k_z=k_F$), both with $\epsilon=\epsilon_F$. The latter wave function penetrates much further into the vacuum and will therefore couple much more strongly to $\phi_{\rm surf}$ than the former. The coupling strength is given by the dimensionless quantity [Eq. (12)]

$$P_{\rm surf}(k_z)=\frac{k_F}{k_z}\,|\langle\psi_{k_z}|Ak_F^2|\psi_{k_z}\rangle|^2 =\frac{k_F}{k_z}\left|\int dz\,|\psi_{k_z}|^2 A(z)k_F^2\right|^2 . \tag{15}$$

Figure 5 shows $P_{\rm surf}(k_z)$, the relative probability for excitation of an electron on the Fermi surface with a given k_z. Obviously, those electrons which propagate normal or almost normal to the surface have the largest probability of being excited.

D. Bulk contribution to Img at zero temperatures

We will now calculate the bulk contribution to $\mathrm{Img}(q_{||},\omega)$ for $q_{||}\ll k_F$ and $\omega\ll\omega_F$. We assume again that the metal can be treated in the jellium approximation (see Fig. 2) and also that the temperature is zero so that there is no contribution from scattering of conduction electrons against phonons.

The rate $w_{\rm bulk}$ at which the potential

$$\phi_{\rm bulk}(\vec{x},t)=\phi_{\rm bulk}(\vec{x})e^{-i\omega t}+\text{c.c.} \tag{16}$$

excites electron-hole pairs in the metal is obtained from the golden-rule formula,

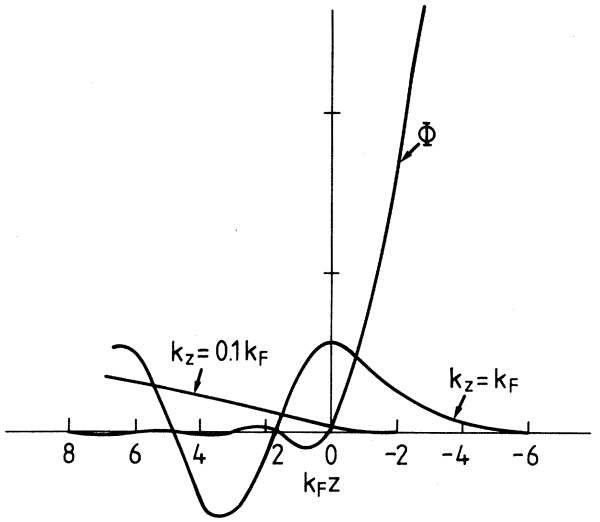

FIG. 4. Potential $\phi_{\rm surf}$ (equal to external plus induced potential) and two electron wave functions $\psi_{k_z}(z)$ ($k_z=0.1k_F$ and k_F), both with $\epsilon=\epsilon_F$, are shown as a function of k_Fz. Electron density parameter $r_s=3$.

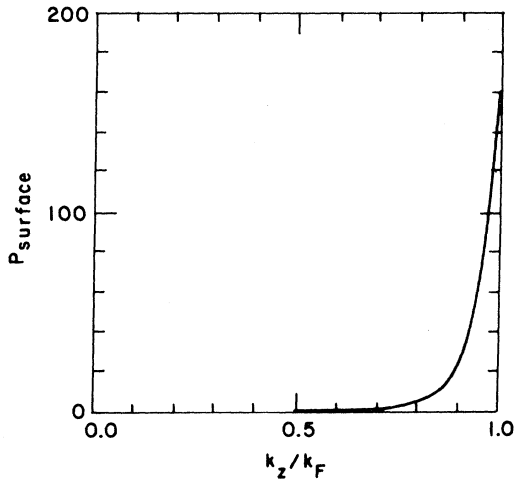

FIG. 5. Relative probability $P_{surf}(k_z)$ for excitation of an electron on the Fermi surface ($\epsilon=\epsilon_F$) as a function of k_z.

$$w_{bulk}=\frac{2\pi}{\hbar}\int d^3k\,d^3k' n_k(1-n_{k'})\,|\langle \vec{k}'\,|\,e\phi_{bulk}(\vec{x})\,|\,\vec{k}\rangle\,|^2 \times\delta(\epsilon_{k'}-\epsilon_k-\hbar\omega)\,. \tag{17}$$

We *assume* now that the potential ϕ_{bulk} for $z>\delta$ is well approximated with

$$\phi_{bulk}(\vec{x})\approx\frac{2\phi_0}{1+\epsilon(\omega)}e^{i\vec{q}_{||}\cdot\vec{x}_{||}-q_{||}z}\,. \tag{18}$$

The metal wave functions for $z>\delta$ are given by

$$\langle\vec{x}\,|\,\vec{k}\rangle=(2\pi)^{-3/2}(e^{i(k_z z+\phi_k)}+e^{-i(k_z z+\phi_k)})\times e^{i\vec{k}_{||}\cdot\vec{x}_{||}}\,. \tag{19}$$

Thus

$$\langle\vec{k}'\,|\,\phi_{bulk}\,|\,\vec{k}\rangle=\frac{2\phi_0}{1+\epsilon}\frac{1}{(2\pi)^3}\int d^2x_{||}e^{i(\vec{k}_{||}+\vec{q}_{||}-\vec{k}'_{||})\cdot\vec{x}_{||}}\int_\delta^\infty dz\,e^{-q_{||}z}(e^{i(k_z z+\phi_k)}+\text{c.c.})(\epsilon^{i(k'_z z+\phi_{k'})}+\text{c.c.})$$

$$=\frac{2\phi_0}{1+\epsilon}\frac{1}{2\pi}\delta(\vec{k}_{||}+\vec{q}_{||}-\vec{k}'_{||})\left[\frac{e^{i(\phi_k-\phi'_k)+(k_z-k'_z)\delta]}}{i(k_z-k'_z)-q_{||}}+\frac{e^{i[(\phi_k+\phi'_k)+(k_z+k'_z)\delta]}}{i(k_z+k'_z)-q_{||}}+\text{c.c.}\right]e^{-q_{||}\delta}\,. \tag{20}$$

Now, since $\delta\sim 1/k_F$ and $q_{||}\ll k_F$, we have $\exp(-q_{||}\delta)\approx 1$. Furthermore, energy and momentum (parallel to the surface) conservation implies that $\vec{k}\approx\vec{k}'$ when $\omega\ll\omega_F$ and $q_{||}\ll k_F$. Thus $\exp[i(\phi_k-\phi'_k)]\approx 1$ and $[q_{||}^2+(k_z-k'_z)^2]^{-1}\gg[q_{||}^2+(k_z+k'_z)^2]^{-1}$. Equation (20) can therefore be written as

$$\langle\vec{k}'\,|\,\phi_{bulk}\,|\,\vec{k}\rangle\approx-\frac{2}{\pi}\frac{\phi_0}{1+\epsilon}\delta(\vec{k}_{||}+\vec{q}_{||}-\vec{k}'_{||})\frac{q_{||}}{q_{||}^2+(k_z-k'_z)^2}\,.$$

Substituting this into Eq. (17) and making use of the formula

$$|\,\delta(\vec{k}_{||})\,|^2=\frac{A}{(2\pi)^2}\delta(\vec{k}_{||})$$

gives

$$w_{bulk}=\frac{2A}{\pi^3\hbar}\left|\frac{e\phi_0}{1+\epsilon}\right|^2\int d^3k\,d^3k' n_k(1-n_{k'})\delta(\vec{k}_{||}+\vec{q}_{||}-\vec{k}'_{||})\delta(\epsilon_k+\hbar\omega-\epsilon_{k'})\frac{q_{||}^2}{[q_{||}^2+(k_z-k'_z)^2]^2}$$

$$=\frac{2A}{\pi^3\hbar}\left|\frac{e\phi_0}{1+\epsilon}\right|^2\frac{m}{\hbar^2}\int d^3k\,n_k(1-n'_k)\frac{1}{k'_z}\frac{q_{||}^2}{[q_{||}^2+(k_z-k'_z)^2]^2}\,, \tag{21}$$

where

$$k'_z=[k^2+2m\omega/\hbar-(\vec{k}_{||}+\vec{q}_{||})^2]^{1/2}$$

$$\approx k_z\left[1+\frac{m\omega^2}{\hbar k_z^2}-\frac{\vec{k}_{||}\cdot\vec{q}_{||}}{k_z^2}\right].$$

We now introduce spherical coordinates in $\vec{k}$ space, with the k_x axis in the $q_{||}$ direction,

$$k_x=k\cos\phi\sin\theta,\quad k_z=k\cos\theta\,.$$

We obtain

$$k'_z-k_z=\frac{1}{k_z}\left[\frac{m\omega}{\hbar}-k_x q_{||}\right]$$

$$=\frac{q_{||}}{\cos\theta}\left[\frac{m\omega}{\hbar k q_{||}}-\sin\theta\cos\phi\right]$$

$$\equiv\frac{q_{||}}{\cos\theta}(\eta-\sin\theta\cos\phi)\,, \tag{22}$$

where

$$\eta=\frac{m\omega}{\hbar k q_{||}}\approx\frac{m\omega}{\hbar k_F q_{||}}=\frac{1}{2}\frac{\omega k_F}{\omega_F q_{||}}\,.$$

Here, the second equality follows from the fact that for $\omega \ll \omega_F$, only $k \approx k_F$ contributes in the integral (21). Substituting (22) into Eq. (21), performing the k integral, and accounting for the electron spin, gives

$$w_{\text{bulk}} = \frac{2A}{3\pi^2} \left| \frac{e\phi_0}{1+\epsilon} \right|^2 \left[\frac{m}{\hbar^2} \right]^2 \frac{\omega}{q_{||}^2} G(\eta) , \tag{23}$$

where

$$G(\eta) = \frac{6}{\pi} \int_0^{\pi/2} d\theta \int_0^{2\pi} d\phi \frac{\sin\theta \cos^3\theta}{[\cos^2\theta + (\eta - \sin\theta\cos\phi)^2]^2} = \frac{3}{\pi} \int_0^1 dx \int_0^{2\pi} d\phi \frac{x}{\{x + [\eta - (1-x)^{1/2}\cos\phi]^2\}^2} , \tag{24}$$

where the last equality follows after the substitution $\cos^2\theta = x$. Since $\text{Img} = \pi\hbar\omega/(|\phi_0|^2 A q_{||})$, we finally obtain

$$(\text{Img})_{\text{bulk}} = (\omega/\omega_p)^2 \eta^3 G(\eta) , \tag{25}$$

where we have replaced

$$1 + \epsilon = 2 - (\omega_p/\omega)^2 \approx -(\omega_p/\omega)^2$$

for $\omega \ll \omega_p$. The function $G(\eta)$ can be calculated analytically,

$$G(\eta) = \begin{cases} 8 & \text{for } \eta < 1 \\ 8[1 - (1 + \frac{1}{2}\eta^{-2})(1-\eta^{-2})^{1/2}] & \text{for } \eta > 1 . \end{cases}$$

Figure 6 shows $G(\eta)$. Note that $G(\eta) \sim 3/\eta^4$ as $\eta \to \infty$. As for the surface contribution, only electrons within a thin shell $\epsilon_F - \hbar\omega < \epsilon < \epsilon_F$ near the Fermi surface can be excited without violating energy conservation. The relative probability $P_{\text{bulk}}(k_z, \eta)$ that an electron in the vicinity of the Fermi surface is excited by ϕ_{bulk} is given by the dimensionless quantity [see Eq. (24) with $\cos\theta = k_z/k_F$]

$$P_{\text{bulk}}(k_z, \eta) = \frac{6}{\pi} \int_0^{2\pi} d\phi \frac{(k_z/k_F)^3}{(k_z/k_F)^2 + \{\eta - [1 - (k_z/k_F)^2]^{1/2}\cos\phi\}^2} .$$

Figure 7 shows this function for a few different $\eta = \omega k_F/(2\omega_F q_{||})$. For $\eta \leq 0.5$, P_{bulk} is almost a constant, while for $0.5 \leq \eta < 1$ it is mainly electrons with small velocity normal to the metal surface that are excited. At $\eta = 1$ there is a steplike change in $P_{\text{bulk}}(k_z = 0)$ from a finite value just below $\eta = 1$ to zero for $\eta > 1$. The relative probability (for $\eta < 1$) for excitation of an electron at the Fermi surface is thus either almost a constant or else it is peaked at small k_z; this is in sharp contrast to the behavior of $P_{\text{surf}}(k_z)$, which is practically zero except in the vicinity of $k_z = k_F$. It is this very different k_z dependence which makes the surface and volume excitation processes almost additive, i.e., $w_{\text{tot}} \approx w_{\text{surf}} + w_{\text{bulk}}$, as pointed out in Sec. II.

E. Comparison with experiments

It is possible to measure $\text{Img}(q_{||}, \omega)$ directly using electron-energy-loss spectroscopy (EELS). In this section it will be shown that there is good quantitative agreement between such measurements and the theory presented in subsections B—D.

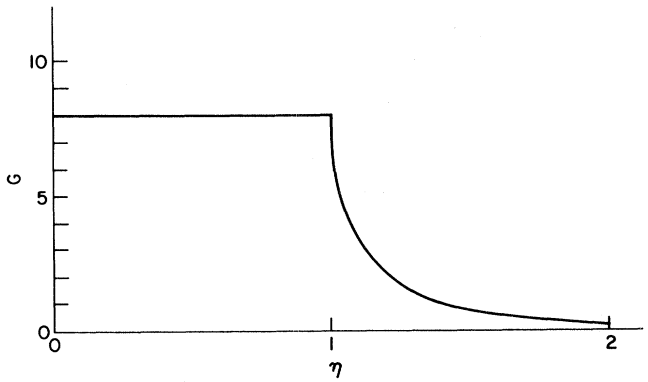

FIG. 6. Function $G(\eta)$ as defined in the text.

We will concentrate our discussion on electron-energy-loss measurements for the clean Cu(100) surface, but we will also present some results for Ni(100). At the low excitation energies investigated, 0.1—0.3 eV, copper can be considered as a reasonably simple metal, e.g., the threshold for the excitation of $3d$-band electrons into the conduction band is at about 2 eV. Below this energy, copper essentially behaves as a free-electron metal. The situation is quite different for nickel where transitions involving $3d$ electrons occur in the low-energy range 0.1—0.3 eV.[10,11] Following standard procedures, the specimens were cleaned initially by argon-ion bombardment and

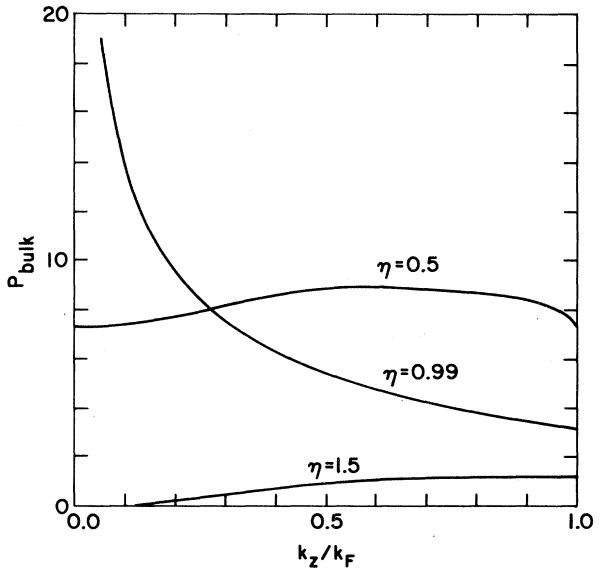

FIG. 7. Relative probability $P_{\text{bulk}}(k_z, \eta)$ for excitation of an electron on the Fermi surface ($\epsilon = \epsilon_F$) as a function of k_z for several different $\eta = \omega k_F/(2\omega_F q_{||})$.

annealing—and between successive measurements by a brief heating to 950 K [Cu(100)] and 1100 K [Ni(100)]—and then cooled to measurement temperature at an ambient pressure in the 10^{-11} Torr range. The surface structure was monitored by low-energy electron diffraction. The EELS measurements reported in this work were obtained with use of a high-resolution spectrometer of cylindrical-mirror construction that has been described elsewhere.[12] Analyzer and specimen can be rotated so that the polar angles of incidence and detection can be varied independently. The scattering plane containing the incident and collected electron beams is defined by the specimen surface normal and the [100] direction in the surface plane. The work-function difference between the spectrometer and the speciment was compensated to within 0.05 eV, and the electron energies quoted refer to the vacuum level. Except for the angular measurements shown in Fig. 8 all spectra were measured in the specular direction. A typical clean Cu(100) spectrum shows, in the energy-loss range 0.1—0.3 eV, a smoothly decreasing intensity (see Fig. 9), and the ratio of loss intensity to elastic intensity is of the order of 10^{-5}—10^{-6}. The spectrum was measured at discrete energy-loss values in order to minimize the measurement time between successive cleanings. A narrow energy window of ± 25 meV around a specific loss energy was recorded and inspected for contributions from any discrete vibrational excitation.

The experimental results discussed below show that the long-range dipole interaction is the predominant mechanism contributing to the inelastic-electron-scattering process. Hence, consider an electron with a few eV energy incident upon a clean metal surface. The electron can be scattered inelastically by the metal while exciting an electron-hole pair in the metal. Let $\vec{k}$ and $\vec{k}'$ denote the wave vector of an incident and an inelastically scattered electron, respectively. Thus $\hbar\vec{q}_{||}$, where $\vec{q}_{||}=\vec{k}_{||}-\vec{k}'_{||}$ is the momentum transfer (parallel to the surface) to the excitation in the metal, and $\hbar\omega=\hbar^2(\vec{k}^2-\vec{k}'^2)/2m$ is the energy transfer. Let $P(\vec{k},\vec{k}')d\Omega_{k'}d\hbar\omega$ be the probability that an incident electron is scattered into the range of energy losses between $\hbar\omega$ and $\hbar(\omega+d\omega)$ and into the solid angle $d\Omega_{k'}$ around the direction of $\vec{k}'$. From standard dipole scattering theory, one has

$$P=\frac{2}{(ea_0\pi)^2}\frac{1}{\cos\alpha}\frac{k'}{k}\frac{1}{q_{||}}|T(\vec{k},\vec{k}')|^2\mathrm{Img}(q_{||},\omega)\ , \tag{26}$$

where α is the angle of incidence, a_0 is the Bohr radii, and

$$T=-\frac{e^{-\pi(\tau+\tau')/2}}{\Gamma(1-i\tau)\Gamma(1-i\tau')}\frac{2\pi\tau'}{1-\exp(-2\pi\tau')}\frac{2ik_z}{k_z'^2}$$
$$\times\int_{-\infty}^{\infty}dw\frac{e^{2i\tau w}}{\sinh^2 w}\left[\frac{\xi+1}{\xi-1}\right]^{i\tau'}\frac{\xi+i\tau'}{(\xi^2-1)^2}\ . \tag{27}$$

Here Γ is the gamma function and

$$\tau=(4k_z a_0)^{-1},\quad \tau'=(4k_z' a_0)^{-1},\quad \xi=-\frac{k_z}{k_z'}\coth w-i\frac{q_{||}}{k_z'}\ .$$

This formula accounts for the force on the incident electron from its own image in the metal. If this force is neglected, one obtains the simpler result[14]

$$T=\frac{q_{||}}{(k_z-k_z')^2+q_{||}^2}-\frac{q_{||}}{(k_z+k_z')^2+q_{||}^2}\ , \tag{28}$$

which, however, is too crude for our purposes.

As discussed earlier, there are three different contributions to Img which can be distinguished by the source of the momentum required for the excitation:

(a) From the bulk: the momentum needed can come from phonons or impurities (i.e., intraband transitions), or from the bulk crystal potential (i.e., interband transitions);

(b) from the surface potential;

(c) from the spatial variation of the potential from the incident electron.

The contribution from (a) is given by the standard textbook result [see Eq. (1)],

$$(\mathrm{Img})_a=\mathrm{Im}\frac{\epsilon(\omega)-1}{\epsilon(\omega)+1}\approx\left[4\frac{\omega_F}{\omega_p}\right]\frac{1}{k_F l}\frac{\omega}{\omega_p}\ , \tag{29}$$

where the last equality is valid if $\epsilon(\omega)$ is well approximated with a Drude dielectric function, $\epsilon\approx 1-\omega_p^2/\omega(\omega+i/\tau)$, and if $1/\tau,\ \omega\ll\omega_p$. l is the mean free path for an electron on the Fermi surface, i.e., $l=v_F\tau$. The contributions from processes (b) and (c) have been calculated in subsections C and D and are, respectively,

$$(\mathrm{Img})_b=2\xi(r_s)\frac{q_{||}}{k_F}\frac{\omega}{\omega_p}\ , \tag{30}$$

$$(\mathrm{Img})_c=\eta^3 G(\eta)(\omega/\omega_p)^2\ , \tag{31}$$

where $\eta=\omega k_F/(2\omega_F q_{||})$, and

$$G(\eta)=\begin{cases}8 & \text{for } \eta<1,\\ 8[1-(1+\frac{1}{2}\eta^{-2})(1-\eta^{-2})^{1/2}] & \text{for } \eta>1\ .\end{cases} \tag{32}$$

The parameter $\xi(r_s)$ depends on the electron-gas—density parameter r_s as shown in Refs. 5 and 7.

Intuitively, one should expect processes (a) and (c) to interfere (i.e., they are not just additive), but we will mainly focus on the zero-temperature limit where the Drude contribution to Img vanishes. We have already shown that there is negligible interference between process (b) and either of processes (a) and (c). Neglecting the interference between (a) and (c) gives

$$\mathrm{Img}=\left[\frac{a}{k_F l}+b\frac{q_{||}}{k_F}+\eta^3 G(\eta)\frac{\omega}{\omega_p}\right]\frac{\omega}{\omega_p}\ , \tag{33}$$

where $a=4\omega_F/\omega_p$ and $b=2\xi$. Treating copper as a free-electron metal with $r_s=2.67$ corresponding to one free electron per Cu atom gives $\xi(r_s=2.67)\approx 0.56$, and $a=2.6$ and $b=1.13$.

The inelastically scattered electrons, as described by (26) and (33), form a narrow lobe centered close to the specular direction. A typical momentum loss of an inelastically scattered electron is $q_{||}\sim k\hbar\omega/(2E_0)$ where E_0 is the energy of the incident electrons. Thus

$$\eta=\omega k_F/(2\omega_F q_{||})\sim E_0 k_F/(E_F k)=k/k_F\ .$$

In most EELS experiments, $E_0<E_F$, and thus $\eta<1$. Consequently, from Eq. (1), $G(\eta)=8$. The relative magni-

tude of the three terms in Eq. (7) is therefore $a/k_F l : bk\hbar\omega/(2k_F E_0) : 8(k/k_F)^3\omega/\omega_p$. With $E_0=3$ eV, $\hbar\omega=0.2$ eV, $r_s=2.67$, and $k_F l=100$, we obtain 2:3:4, i.e., processes (b) and (c) already dominate at room temperature. At lower temperatures the difference is even larger because $l\to\infty$ as $T\to 0$ K. By studying the intensity of the inelastically scattered electrons as a function of temperature, it is possible to separate the Drude contribution $(\mathrm{Im}g)_a$ from the other contributions, as will be seen below. The experimentally measured inelastic scattering probability ΔP relates simply to $P(\vec{k},\vec{k}')$ integrated over the solid angle of detection $\Delta\Omega$,

$$\Delta P=\int_{\Delta\Omega} P(\vec{k},\vec{k}')d\Omega_{\vec{k}'}.$$

In the present case $\Delta\Omega$ consists of a circular aperture of half angle 0.45°. The angular distributions for elastically and inelastically (0.1 and 0.3 eV energy loss) scattered electrons from Cu(100) are shown in Fig. 8. A narrow energy window of ±25 meV around the specific loss energy was recorded and inspected for any contribution from discrete vibrational excitations related to surface contamination. The specimen temperature is 293 K and the energy of the incident electrons is 2.3 eV. The elastic intensity distribution (solid curve) is symmetrical around the specular direction $\theta=0$, and has a full width at half maximum of 0.90°. The two inelastic intensity distributions show broader peaks with maxima centered close to the specular direction, and the widths relate approximately as the corresponding loss energies. These are characteristic features for dipole-excited transitions and the inelastic scattering apparently takes place via the long-range dipole interaction. Figure 9 shows how the inelastic scattering probability ΔP for Cu(100) depends on the loss energy $\hbar\omega$. The inset shows the measured data for ΔP at $\hbar\omega=0.1$, 0.15, 0.2, and 0.3 eV, and for several temperatures. The data were obtained at discrete loss energies in the way described above. We note that ΔP varies linearly with temperature, which is also expected from optical data for copper.[15] This is also the prediction, from standard theory, of the phonon resistivity[16] for $T>0.2T_D$ (where T_D is the Debye

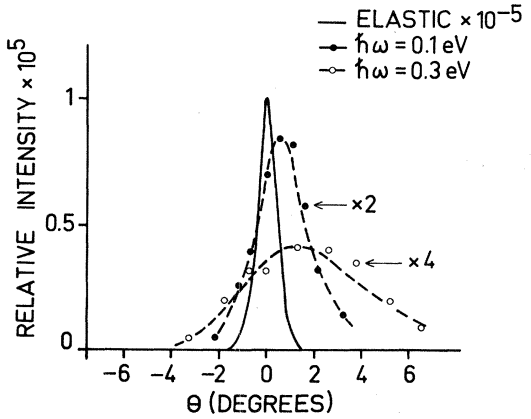

FIG. 8. Experimental elastic and inelastic ($\hbar\omega=0.1$ and 0.3 eV) intensity vs collection angle θ ($\theta=0°$ specular and $\theta>0°$ towards surface normal) scattered from Cu(100) at 293 K. Energy of incident-electron beam, 2.3 eV; angle of incidence, 54°.

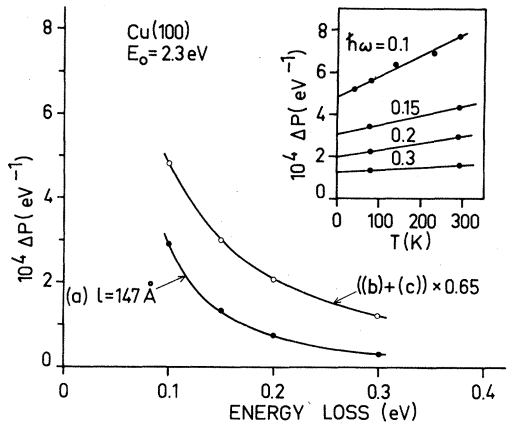

FIG. 9. Inelastic scattering probability ΔP vs loss energy $\hbar\omega$ and temperature T (see inset) for 2.3-eV electrons; specular condition. The open and solid circles represent the extrapolated experimental $\Delta P(T=0\text{ K})$ and $\Delta P(T=293\text{ K})-\Delta P(T=0\text{ K})$ data respectively. The solid curves are the theoretically predicted results for process (a), and (b) + (c), respectively (see text).

temperature). The open circles in Fig. 9 correspond to the ΔP values obtained by extrapolating the data in the inset to $T=0$ K. The solid circles show the Drude contribution to ΔP at room temperature as given by $\Delta P(T=293\text{ K})-\Delta P(T=0\text{ K})$. The solid curves are theoretically predicted results for the ΔP for processes (b) + (c) [Eqs. (30) and (31)] and (a) [Eq. (29)] using $l=147$ Å. We note that there is an almost perfect agreement between theory and experiment with respect to the dependence of ΔP on the loss energy $\hbar\omega$. The mean free path compares favorably with the value of 125 Å deduced from optical data for Cu.

The absolute value of ΔP deviates by only 35% from the theoretical result, and on the average by less than 20% over a range of impact energies, as can be seen in Fig. 10. The open and solid circles correspond to experimental

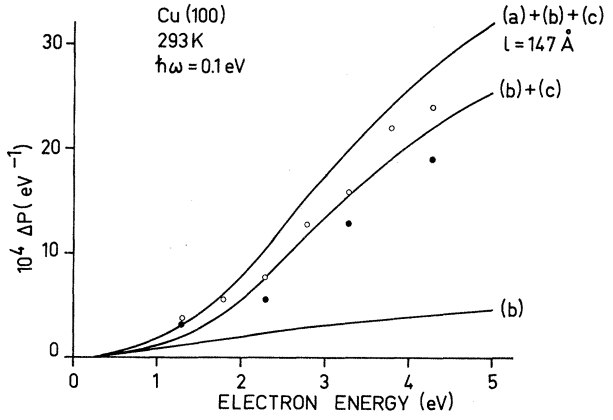

FIG. 10. Inelastic scattering probability ΔP vs incident-electron energy. The open and solid circles denote the experimental ΔP values at $T=293$ and 80 K, respectively, for 0.1-eV loss energy and specular condition. The solid curves are the calculated results for processes (b), (b) + (c), and (a) + (b) + (c), respectively (see text).

data for $\hbar\omega = 0.1$ eV obtained at 293- and 80-K substrate temperature, respectively. The solid curves correspond to the calculated contributions from processes (a) + (b) + (c), (b) + (c), and (b), respectively. The Drude contribution (a) at $T = 293$ K was calculated for $l = 147$ Å, as found above. The agreement between experiment and theory [the $T = 293$ K experimental data should be compared with processes (a) + (b) + (c)] is very good, in terms of what concerns the dependence of ΔP on the incident electron energy, the absolute value of ΔP, and the relative magnitude of the Drude contribution. The importance of the (c) contribution is obvious from Fig. 10. The agreement between the experimental data for a copper surface and the predicted result for a jellium surface is in fact surprisingly good. Copper is not a perfect free-electron metal; for example, both the work function [which affects process (b)] and the effective electron mass [which affects processes (b) and (c)] differ from the prediction of the jellium model, and this must be accounted for in a more accurate model.

Figure 11 shows ΔP as a function of the loss energy $\hbar\omega$ for Ni(100). The open and solid circles show the experimental data at $T = 293$ and 80 K, respectively. The solid angle of detection $\Delta\Omega$ consists of a circular aperture of half-angle 0.65°. The solid lines show the theoretically predicted results for processes (a) and (b) + (c), respectively. In the calculation of curve (a) we have used the measured dielectric function (at $T = 293$ K), and in calculating curves (b) and (c) we have used the jellium model with one free electron per Ni atom. Ni is, of course, less well represented by a jellium model compared with Cu. Ni has a partially unfilled $3d$ band which is manifested in the experimental data and in curve (a) by an interband transition[10,11] at $\hbar\omega \simeq 0.2$ eV. It is plausible to assume, however, that process (b) is reasonably well described by the jellium result, while process (c) certainly should be described by a more appropriate $\epsilon(\omega)$. We notice, however, that the absolute magnitude of the experimental ΔP agrees quite well with the sum of (a) and (b) + (c).

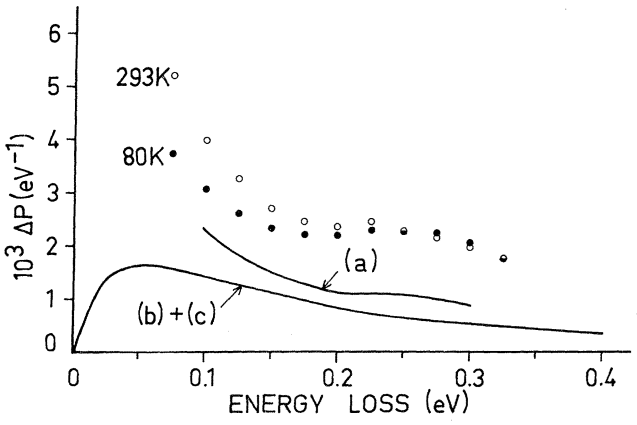

FIG. 11. Inelastic scattering probability ΔP for Ni(100) vs loss energy $\hbar\omega$ for 2.3-eV electrons; specular condition. The open and solid circles are the experimental data at $T = 293$ and 80 K, respectively. The solid curves are the theoretically predicted results for process (a) and (b) + (c), respectively (see text).

F. Some comments

The basic assumption behind the derivation of $(\mathrm{Img})_c$ in subsection D was that the total potential $\phi(\vec{x}t)$ for $z > \delta$ is well approximated by the "classical" result (18). This assumption is certainly correct if, for a fixed frequency ω, $q_{||}$ is small enough ($q_{||} \ll k_F\omega/\omega_F$). Here one utilizes the fact that the bulk dielectric function $\epsilon(k,\omega) \to \epsilon(\omega)$ as $k \to 0$. Stated another way, for sufficiently long wavelengths, all the oscillator strength is carried by the plasmon. However, for $q_{||} \gtrsim k_F\omega/\omega_F$, excitation of electron-hole pairs will give a contribution to the screening of the external potential which is not accounted for when using the long-wavelength limit $\epsilon(\omega)$ of the bulk dielectric function. Thus it is not obvious from a theoretical point of view how accurate formula (25) is. The strongest support for (25), being at least a reasonable first approximation, comes instead from the analysis of the experimental data in the preceding subsection. In particular, the good agreement between theory and experiment for the Drude contribution $(\mathrm{Img})_a$ indicates that the electric potential inside the metal must be quite similar to the classical result (18). If, for example, electron-hole—pair excitations would give such a large contribution to the screening that the potential vanished inside the metal as $\exp(-az)$ where $a \sim k_F$ instead of $a \sim q_{||}$, then the Drude contribution to $(\mathrm{Img})_a$ would be much smaller, and, more importantly, it would have a different dependence on the loss energy $\hbar\omega$ [it would depend on $\hbar\omega$ in the same way as the surface contribution $(\mathrm{Img})_b$]. However, the agreement between theory and experiment for $(\mathrm{Img})_a$, with respect to the dependence on $\hbar\omega$, is almost perfect.

Finally, let us comment on the magnitude of the mean free path l. In subsection E we deduced that $l \sim 147$ Å, and similar values can be deduced from infrared-light-reflection measurements. However, from d.c.-conductivity measurements, $l \sim 400$ Å, almost a factor of 3 longer mean free path. Thus the Drude relaxation time for small frequencies is, in general, different from the Drude relaxation time occurring in the static conductivity.[17]

III. APPLICATION

A. Total cross section for inelastic scattering of charged particles from metal surfaces

The energy transfer between a beam of charged particles and a metal is a subject with many important applications in the areas of sputtering[18] and ion-beam etching[19] of semiconductors. Here we will briefly discuss the energy transfer between low-energy electrons and a metal. This is, of course, exactly the same problem as that discussed in Sec. II E, but in that subsection we presented no results for the total inelastic scattering cross section, which we will do now.

Consider a beam of monoenergetic electrons incident upon a clean metal surface. Let α be the angle of incidence and let E_0 denote the kinetic energy of an electron when it is far away from the surface (it will speed up as it comes closer owing to the electron-image—electron in-

teraction). In classical (Newtonian) mechanics, the probability than an incident electron scatters elastically from the surface is exactly zero. On the contrary, in quantum mechanics there is always a finite probability for elastic scattering. Thus if A denotes this probability, we can write the relative probability $P(\hbar\omega)$ that an electron loses the energy $\hbar\omega$ to an excitation in the metal as

$$P(\hbar\omega)=A\delta(\hbar\omega)+B(\hbar\omega) .$$

The function $B(\hbar\omega)$ is obtained as

$$B(\hbar\omega)=\int_{k_z'\geq 0} d\Omega_{k'} P(\vec{k},\vec{k}') , \tag{34}$$

where $P(\vec{k},\vec{k}')$ is the relative probability for an electron to be inelastically scattered from $\vec{k}\rightarrow\vec{k}'$ (see Sec. II E). The integral is over the solid angle of the whole upper half-space.

In Figure 12 we show $P(\hbar\omega)$ for $E_0=1.5$ and 3 eV with $\alpha=45°$. The metal is, as before, treated within the jellium model ($r_s=2.67$). The solid curves give $B(\hbar\omega)$ as obtained from Eq. (34) with $P(\vec{k},\vec{k}')$ given by Eq. (26), and the weight A of the elastic peak was obtained from the conservation of probability

$$1=\int d\hbar\omega\, P(\hbar\omega)=A+\int d\hbar\omega\, B(\hbar\omega) .$$

The results presented here must be taken with some reservation because the expression for $\mathrm{Img}(q_{||},\omega)$ that we have used is only valid for small $q_{||}$ and ω ($q_{||}\ll k_F$ and $\omega\ll\omega_F$), and since, e.g., $\hbar\omega_F=7$ eV for $r_s=2.67$, the inequality $\hbar\omega\ll\hbar\omega_F$ is not very well satisfied with $\hbar\omega\sim 3$ eV. The dashed curves denoted (c) in the figure are, as usual, the contribution from the electric field in the bulk. The solid curve is the result obtained by adding the surface contribution to Img. We note here that at these low energies of the incident electrons, it is important to account for the image force on the incident electron. Neglecting this image increases $B(\hbar\omega)$ by typically a factor of 2.

In the presented calculation of A we have neglected processes where the incident electron is scattered inelastically into a bound state in the image potential. The cross section for these processes is actually contained in formula (26) if one performs an analytical continuation of the "T matrix" given by Eq. (27) to complex k_z' values. The bond states will then occur at poles of the T matrix. Indeed, from Eq. (27) we note that $T(\vec{k},\vec{k}')$ has poles when $\Gamma(\tau')[1-\exp(-2\pi\tau')]/\tau'=0$, i.e., $\tau'=in$, $n=1,2,\ldots$. But since $k_z'=1/(4a_0\tau')$ we obtain

$$E_n=\hbar^2k_{||}'^2/2m+\hbar^2k_z'^2/2m=\hbar^2k_{||}'^2/2m-\hbar^2/(32ma_0^2n^2) ,$$

i.e., the expected Rydberg series.

Figure 12 shows that the inelastic scattering probability

$$\int d\hbar\omega\, B(\hbar\omega)=1-A$$

is a small fraction of unity. That is almost all the electrons in the incident beam are elastically scattered. It is a consequence of this that lowest-order perturbation theory [on which formula (27) is based] is a good approximation in the present case.

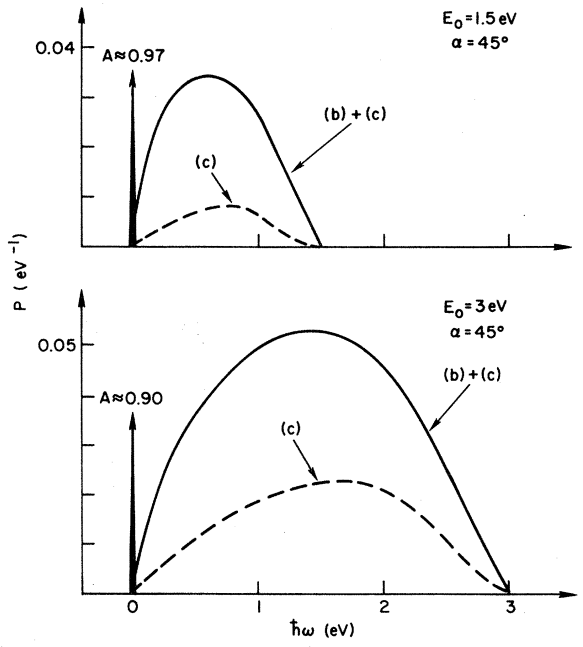

FIG. 12. Relative loss probability $P(\hbar\omega)$ as a function of the loss energy $\hbar\omega$. The incident electrons have the kinetic energy $E_0=1.5$ eV (top) and 3 eV (bottom), and the angle of incidence $\alpha=45°$. Electron-gas density parameter $r_s=2.67$.

Imagine now that it would be possible to continuously increase the electron mass $m\rightarrow M>m$. Assume also that E_0 is so large that it is possible to neglect the force on the incident electron from its own image in the metal. It is then easy to see from Eqs. (26), (28), and (33) that the inelastic scattering probability for a fixed E_0 increases as $(M/m)^{1/2}$ for process (a), as M/m for process (b), and decreases as $(M/m)^{-3/2}$ for process (c). Thus, when M becomes large enough, the inelastic scattering probability will formally become larger than unit which, of course, implies that Eq. (27) breaks down. Mathematically this means that it is not enough to use first-order perturbation theory but one has to include further terms in the perturbation expansion. Physically it means that for large enough M/m, an incident electron will, in general, undergo multiple scattering, i.e., it will excite several electron-hole pairs in the metal. Actually, in the limit $M\rightarrow\infty$ (for fixed E_0) an infinite number of low-energy electron-hole pairs will be excited in the substrate, as is schematically shown in Fig. 13. The interaction with the metal is now so frequent that we have entered into the Brownian-motion regime. Here one treats the particle as a classical point particle acted upon by a frictional force $\vec{f}$,

$$\vec{f}=-\eta_\perp\vec{v}_\perp-\eta_{||}\vec{v}_{||} ,$$

caused by the interaction with the metal. In principle, not only electron-hole pairs, but also phonons, should give a contribution to the friction parameters $\eta_\perp$ and $\eta_{||}$ for orthogonal and parallel motion. It is easy to show that[20] $\eta_{||}=\eta_\perp/2$. It is possible[21] to derive an expression for $\eta_\perp$ by simply considering the energy loss due to friction (the work done against f) of a particle of charge $+Q$ and mass

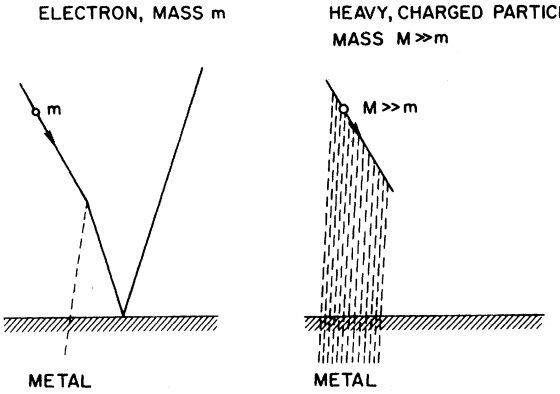

FIG. 13. A low-energy electron (E_0 of approximately a few eV) has a negligible probability to excite more than one electron in the metal. A very heavy particle (e.g., a proton) with the *same* kinetic energy will on the average excite many electron-hole pairs in the metal.

M executing infinitesimal oscillations against a stationary particle of charge $-Q$,

$$\frac{M\eta_\perp}{Q^2}=\lim_{\omega\to 0}\frac{1}{8\omega d^3}\int_0^\infty d\zeta\,\zeta^2 e^{-\zeta}\mathrm{Im}g(\zeta/2d,\omega)\,.$$

The integral in this expression is identical to that in the expression for the damping of a vibrating point dipole, Eq. (36), and in the next section it will be shown that

$$\frac{M\eta_\perp}{Q^2}=\frac{1}{8\omega d^3}\frac{1}{k_F d}\kappa_b\,,$$

where we have neglected the Drude contribution, which gives a negligible contribution in most cases. Note also that there is no contribution from $(\mathrm{Im}g)_c$ since $\omega^{-1}(\mathrm{Im}g)_c\to 0$ as $\omega\to 0$.

As an illustration, let us consider a proton with the kinetic energy $E_0=10^3$ eV moving normally to the metal. The energy transfer from the proton to the metal during the trip from $z=-\infty$ to $-d$ is easily obtained as

$$\int_{-\infty}^{-d} f_z dz=\frac{Q^2}{d}\frac{1}{k_F d}\frac{v_z}{3\omega_p d}\kappa_b\sim 1\text{ eV}\,,$$

if $d\sim 1$ Å (actually, the present theory is only valid for $q_{||}\gg k_F$, i.e., $k_F d\gg 1$ and the value given here for $d\sim 1$ Å is probably an overestimate of the real energy transfer). Thus the total energy transfer is almost 0.1% or so of the original kinetic energy of the proton. Of course, when the proton penetrates into the substrate much more complicated processes will occur involving much larger energy transfer.

B. Electron-hole–pair quenching of excited states near a metal

In recent years there has been a growing interest in understanding the nature and decay mechanisms of electronic and vibrational excitations of adsorbates. Such information is important in a variety of research areas such as photon and electron-stimulated desorption,[23] photoluminescence[23] and photochemistry[24] of adsorbates, resonance photoemission,[25] and the surface-enhanced Raman effect.[26]

Consider a vibrationally or electronically excited molecule located a distance d above a metal surface. The excited molecule can decay (with a lifetime τ^*) to its ground state either by spontaneous emission of a photon (fluorescence) or by nonradiative transfer of the excitation energy to the metal. The latter process is known to be the dominating channel if $d<c/\Omega$, where $\hbar\Omega$ is the excitation energy of the molecule. In what follows we will only consider nonradiative decay processes.

Assume that we can treat an excited molecule as a vibrating point dipole. The electric field from the vibrating dipole penetrates into the metal where it can excite electron-hole pairs. It has been shown elsewhere that the damping rate for a dipole vibrating normal to the surface is given by[28]

$$\frac{1}{\tau^*}=\frac{|\langle B|\hat{\mu}|A\rangle|^2}{4d^3\hbar}F(\Omega,d)\,,\tag{35}$$

where

$$F=\int_0^\infty d\zeta\,\zeta^2 e^{-\zeta}\mathrm{Im}g(\zeta/2d,\Omega)\,,\tag{36}$$

where $\langle B|\hat{\mu}|A\rangle$ is the matrix element of the dipole-moment operator between the ground state $|A\rangle$ and the excited state $|B\rangle$. The Drude contribution to the damping rate is obtained by substituting

$$(\mathrm{Im}g)_a=\mathrm{Im}\frac{\epsilon(\omega)-1}{\epsilon(\omega)+1}\approx 4(\omega_f/\omega_p)\frac{1}{k_F l}\frac{\omega}{\omega_p}$$

into Eq. (36),

$$F_a=2\,\mathrm{Im}\frac{\epsilon(\omega)-1}{\epsilon(\omega)+1}\approx 8(\omega_F/\omega_p)\frac{1}{k_F l}\frac{\omega}{\omega_p}\,.\tag{37}$$

The resulting formula for the damping rate, obtained by combining Eqs. (35) and (37), is well known[27] and will probably give the correct damping rate for large d (but $d<c/\Omega$). The surface contribution to the damping rate is obtained by substituting

$$(\mathrm{Im}g)_b=2(q_{||}/k_F)(\omega/\omega_p)\xi$$

into Eq. (36). We have

$$F_b=2\xi\frac{\omega}{\omega_p}\frac{1}{2k_F d}\int_0^x d\zeta\zeta^3 e^{-\zeta}=6\xi\frac{\omega}{\omega_p}\frac{1}{k_F d}\,.\tag{38}$$

This formula is valid for large d (i.e., small $q_{||}$) and small ω. Finally, the damping due to process (c) at zero temperature ($k_F l=\infty$) is for $\omega\ll\omega_p$ obtained by substituting $(\mathrm{Im}g)_c=(\omega/\omega_p)^2\eta^3 G(\eta)$ into Eq. (36),

$$F_c=(\omega/\omega_p)^2 f(\omega k_F d/\omega_F)\,,\tag{39}$$

where

$$f(x)=8x^3\int_0^1 d\mu\frac{1}{\mu}[1-(1+\tfrac{1}{2}\mu^2)(1-\mu^2)^{1/2}]e^{-\mu x}+8x^3\int_1^\infty d\mu\frac{1}{\mu}e^{-\mu x}$$

is obtained after introducing the new integration variable $\mu=\zeta/x$. Figure 14 shows $f(x)$. It is easy to show that

$$f\sim 18/x \quad \text{as } x\to\infty, \quad f\sim -8x^3\ln x \quad \text{as } x\to 0 .$$

Thus as $k_F d\to\infty$ for a fixed ω we obtain

$$F_c = 18\frac{\omega}{\omega_p}\frac{\omega_F}{\omega_p}\frac{1}{k_F d} ,$$

which depends on ω and $k_F d$ in the same way as F_b. For $k_F d\to\infty$ we can therefore write

$$F_b+F_c=\frac{\omega}{\omega_F}\frac{1}{k_f d}(\kappa_b+\kappa_c) , \tag{40}$$

where $\kappa_b=6\xi$ and $\kappa_c=18\omega_F/\omega_p$. Figure 15 shows κ_b and κ_c as a function of the electron-gas–density parameter r_s.

It is interesting to compare the classical Drude contribution to the damping rate, as given by Eq. (37), with the contribution from process (b) and (c) as given by Eq. (40). Obviously, both are linear, in ω (for small ω) but they have a different distance dependence; $1/\tau_a^*\sim 1/d^3$ while $1/\tau_{b+c}^*\sim 1/d^4$. For a more detailed discussion of the relative importance of F_a as compared with F_b, we refer the reader to Ref. 7 [note, however, that Ref. 7 does not account for process (c)]. In Ref. 7 it was suggested[28] that one should measure the lifetime of an excited molecule located at various distances above a metal surface and determine whether the lifetime varies as d^3 or d^4. In the case of a silver and with an excitation energy below the onset of transitions from the d band, i.e., $\hbar\omega\lesssim 3$ eV, the mean free path l is very long, $l\sim 300$ Å. Thus F_b+F_c should dominate even for large d because from Eqs. (37) and (40) $F_{b+c}\approx 3d/l$ for $r_s=3$. Experiments to test these theoretical predictions are now under progress.[29]

IV. SUMMARY

We have presented a simple model calculation of the response of a jellium metal surface to an external electric field varying slowly in space and time. The discussion focused on $g(q_{||},\omega)$, which is the reflection factor for an evanescent p-polarized plane wave. This linear-response function determines the influence of a metal surface on all dynamical processes occurring outside of it. We illustrated this in Sec. III by applications to the friction force on a charged particle and the damping of vibrations at surfaces. The review article by Feibelman[8] contains many other applications to, e.g., the surface photoelectric effect, the surface power absorption, and the dynamical image-plane position.

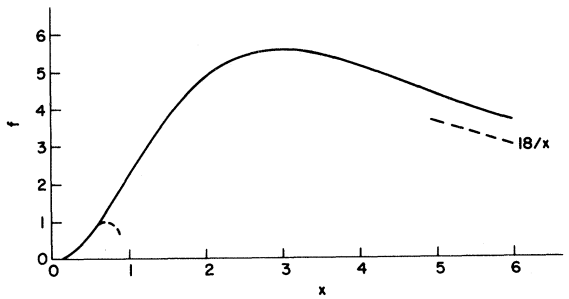

FIG. 14. Function $f(x)$ is defined in the text.

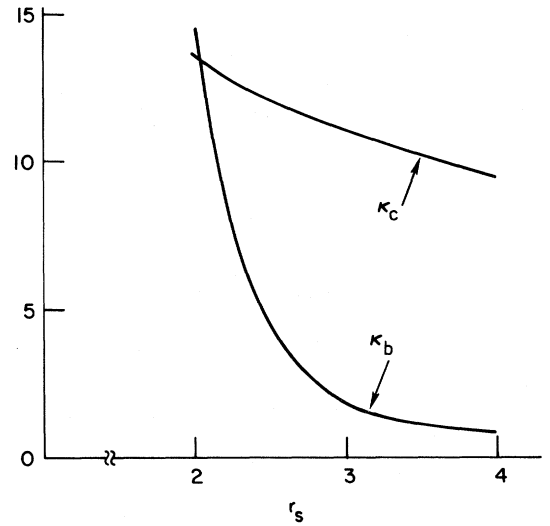

FIG 15. κ_b and κ_c as functions of the electron-gas–density parameter r_s.

The quantity $\mathrm{Im}g(q_{||},\omega)$ is proportional to the power absorption in the metal caused by an external potential of the form $\phi_{\text{ext}}\sim e^{i(\vec{q}_{||}\cdot\vec{x}_{||}-\omega t)-q_{||}z}$. In Secs. II C–II D Img was calculated within the jellium model and for $q_{||}\ll k_F$ and $\omega\ll\omega_p$. The result can be summarized as follows: In the excitation of an electron-hole pair in the metal, both energy and momentum must be conserved. The energy from the external potential but the momentum can come from various sources, namely the following:

(a) From the bulk: the momentum needed can come from phonons or impurities (i.e., intraband transitions), or from the bulk crystal potential (i.e., interband transitions);
(b) From the surface potential;
(c) From the spatial variation of the external potential.

The results presented in Sec. II showed that the contributions from processes (b) and (c) often dominates over the classical contribution (a), particularly at low temperatures. Thus the standard textbook treatment of optics of metals, which only accounts for process (a), will fail for frequencies in the infrared region, even for quite small $q_{||}$ (for instance, $q_{||}\sim 10^{-2}$ Å^{-1}). For higher frequencies the contribution from process (a) might dominate, particularly for transition metal where interband transitions occur.

In Sec. II F the theoretical results for Img were compared favorably with inelastic-electron-scattering measurements on Cu(100) and Ni(100).

We emphasize that the theoretical discussion presented in Sec. II is based on a few plausible assumptions which, however, should be tested by more accurate calculations along the lines of Feibelman.[8] In particular, the assumption behind the treatments of processes (a) and (c), namely

that the electric potential well inside the metal takes the classical bulk form [Eq. (19)], and also that any interference between processes (a) and (c) can be neglected, deserves a more detailed study.

Noted added in proof. We have studied the interference term between processes (b) and (c) and found that this contribution, in general, is non-negligible [E. Zaremba and B. N. J. Persson, (unpublished)].

[1]J. E. Demuth, H. Ibach, and S. Lehwald, Phys. Rev. Lett. 40, 1044 (1978).

[2]B. N. J. Persson and R. Ryberg, Phys. Rev. Lett. 48, 549 (1982).

[3]See, e.g., B. I. Lundqvist, H. Hjelmberg, and O. Gunnarsson, in *Photoemission and the Electronic Properties of Surfaces,* edited by B. Feuerbacher, B. Fitton, and R. F. Willis (Wiley, New York, 1978), Chap. 9.

[4]E. Zaremba and W. Kohn, Phys. Rev. B 13, 2270 (1976); 15, 1769 (1977).

[5]B. N. J. Persson and P. Apell, Phys. Rev. B 27, 6058 (1983).

[6]See, e.g., A. Campion, A. R. Gallo, C. B. Harris, H. J. Robota, and P. M. Whitmore, Chem. Phys. Lett. 73, 447 (1980).

[7]B. N. J. Persson and N. D. Lang, Phys. Rev. B 26, 5409 (1982).

[8]P. J. Feibelman, Prog. Surf. Sci. 12, No. 4 (1982); Phys. Rev. B 22, 3654 (1980); 12, 1319 (1975); 14, 762 (1976).

[9]H. J. Levinson, E. W. Plummer, and P. J. Feibelman, Phys. Rev. Lett. 43, 952 (1979).

[10]D. W. Lynch, R. Rosei, and J. H. Weaver, Solid State Commun. 9, 2195 (1971).

[11]H. Ibach and S. Lehwald, Solid State Commun. 45, 633 (1983).

[12]S. Andersson, in *Vibrations at Surfaces,* edited by R. Caudano, J. M. Gilles, and A. A. Lucas (Plenum, New York, 1982), p. 169.

[13]B. N. J. Persson, Surf. Sci. 92, 265 (1980).

[14]H. Ibach and D. L. Mills, *Electron Energy Loss Spectroscopy and Surface Vibrations* (Academic, New York, 1982); D. L. Mills, Surf. Sci. 48, 59 (1975); E. Evans and D. L. Mills, Phys. Rev. B 5, 4126 (1972); D. M. Newns, Phys. Lett. 60A, 461 (1977); F. Delanaye, A. Lucas, and G. D. Mahan, Surf. Sci. 70, 629 (1978); B. N. J. Persson, Solid State Commun. 24, 573 (1977); D. Sokceric, Z. Lenac, R. Brako, and M. Sûnjić, Z. Phys. B 28, 677 (1977); W. L. Schaich, Phys. Rev. B 24, 686 (1981).

[15]P. B. Johnson and R. W. Christy, Phys. Rev. B 11, 1315 (1975).

[16]A. H. Wilson, *The Theory of Metals* (Cambridge University Press, Cambridge, England, 1965).

[17]J. B. Smith and H. Ehrenreich, Phys. Rev. B 25, 923 (1982).

[18]G. E. Thomas, Surf. Sci. 90, 381 (1979).

[19]*Desorption Induced by Electronic Transitions, Springer Series in Chemical Physics,* edited by N. H. Tolk, M. M. Traum, J. C. Tully, and T. E. Madey (Springer, New York, 1983).

[20]J. Harris and R. O. Jones, J. Phys. C 7, 3751 (1974).

[21]W. L. Schaich (private communication); B. N. J. Persson and W. L. Schaich, J. Phys. C 14, 5583 (1981).

[22]D. Menzel, J. Vac. Sci. Technol. 20, 538 (1982).

[23]G. Ritchie and E. Burstein, Phys. Rev. B 24, 4843 (1981).

[24]G. M. Goncher and C. B. Harris, J. Chem. Phys. 77, 3767 (1982); A. Nitzan and L. E. Brus, *ibid.* 75, 2205 (1981).

[25]B. E. Koel, G. M. Loubriel, M. L. Knotek, R. H. Stulen, R. A. Rosenberg, and C. C. Parks, Phys. Rev. B 25, 5551 (1982).

[26]For recent reviews, see *Surface Enhanced Raman Scattering,* edited by R. K. Chang and T. E. Furtak (Plenum, New York, 1982); A. Otto, in *Light Scattering in Solids,* edited by M. Cardona and G. Güntherodt (Springer, Berlin, 1983).

[27]H. Morawitz, Phys. Rev. 187, 1792 (1969); R. R. Chance, A. Prock, and R. Silbey, Adv. Chem. Phys. 37, 1 (1978), and references therein; B. N. J. Persson, J. Phys. C 11, 4251 (1978).

[28]Many experiments of this kind have been reported in the literature, but never performed under such conditions that the surface damping dominates. Thus, for example, Campion *et al.* [Chem. Phys. Lett. 73, 447 (1980)] studied a pyrazine ($\hbar\Omega = 3.3$ eV) -nickel system. They found that $r \sim d^3$ for $50 > d > 8$ Å, as expected for bulk damping. Owing to the short mean free path for electrons in Ni ($k_F l \sim 1$), this result is expected. For other lifetime measurements, see K. H. Drexhage, M. Fleck, H. Kuhn, F. P. Schäfer, and W. Sperling, Ber. Bunsenges. Phys. Chem. 73, 1179 (1969); I. Pockrand, A. Brillante, and D. Möbius, Chem. Phys. Lett. 69, 499 (1980); J. E. Demuth and Ph. Avouris, Phys. Rev. Lett. 47, 61 (1981). See also the work of the Ford group [Opt. Lett. 4, 236 (1979) and Chem. Phys. Lett. 75, 274 (1980)], as well as H. Morawitz [NATO Adv. Study Inst., Ser. B 37, 261 (1978)] and P. M. Withmore, A. P. Alivisatos, and C. B. Harris [Phys. Rev. Lett. 50, 1092 (1983)].

[29]A. P. Alivisatos and C. B. Harris (private communication); W. Krasse (private communication).